

## Bidirectional Multiple Negative Differential Resistance (BM-NDR): A Theoretical Study of Molecular Device

Certainly, we as scientific community are not blessed with abundant resources to carry out all the research activities experimentally. Therefore, computational methods were developed to predict the nature of particles. One such method among others is based on quantum mechanical effects and its equations determine the electrical and physical properties of molecules. In this chapter our prime goal will be to illustrate the electrical properties of a single molecule two terminal device. The mass production of single molecule devices is yet a challenge for researchers and engineers. Therefore, the identification of the potential of a molecule apriori based on its application will certainly prepare a database of the molecules of the future electronics devices. In the attempt to achieve this, 2,3-Dichloro-5,6-dicyano-1,4-benzoquinone (DDQ), a molecule from quinone family with two oxygen atoms, two chlorine atoms and two cyanide groups was chosen. The following study has already been published (Dagar et al., 2019).

### 4.1 Introduction

With the advent of molecular electronics, which started with the idea of understanding a basic diode structure using organic molecule (Aviram and Ratner, 1974), a completely alternate world of electronics came into existence. Came along a myriad of other molecular electronic devices such as single molecule transistors (Liang et al., 2002), molecular switching devices (Pease et al., 2001), molecular rectifiers (Dhirani et al., 1997), etc. The inspiration for using single molecule as active component in electronic devices came from the challenge of further miniaturization of the electronic devices using CMOS technology. One of the problems in miniaturization is reliability of the device operation, which can be in principle addressed using molecular electronics. One of the fascinating characteristics that was studied over the years is negative differential resistance (NDR). The reason for studying the device is the array of device applications such as memory logic circuits (Mathews et al., 1999), oscillator (Chow et al., 1992), Analog to Digital (A/D) converter (Broekaert et al., 1998). Much of experimental and theoretical work have gone into the understanding of this device, but because of the ambiguous nature of its explanations, it is still under extensive research. From various explanations of the experimental observations on this effect, one stands out explanation was given by Chen et al. (Chen et al., 1999) where for a self-assembled monolayer (SAM) of a molecule the NDR was due to the double reduction of the molecule by the injected electrons from the electrode.

Theoretically NDR was explained by using various models. One of the models suggests that charging of the molecule causes torsion in the central aromatic ring in the molecule (Seminario et al., 2000). The charging of the molecule changes the HOMO-LUMO gap (HLG) of the molecule, which eventually causes momentary hindrance in charge transport. In another work it was explained on the basis of the interaction by the interface states between the electrode and molecule which are spread to the electrode side (Dalglish and Kirczenow, 2006). The importance of orientation of the crystallographic planes in the electrode is also taken into consideration. Some researchers have used a molecular double dot model of two molecules where the molecular level crossing is believed to be the reason for NDR effect (Liu et al., 2006). A room

temperature NDR was explained by considering the resonant tunneling between the localized states in the electrode and the molecule (Guisinger et al., 2004b), molecule and molecule (Zheng et al., 2010), or in some other instances a redox reaction preceding a resonant tunneling (Mentovich et al., 2008). A spatial resonance and local symmetry matching of the electronic bands in different parts of the device was also used to conceptualize the idea of NDR (Chen et al., 2007a). For some donor acceptor based molecular electronic devices which showed NDR, it was explained by considering the PDOS profile of both molecule and electrodes and if they match then only NDR is possible (Geng et al., 2007). In fact, for a bimolecular device configuration the NDR was shown to be due to the splitting of the frontier orbitals within the bias window, which is a result of the molecular interaction (Long et al., 2007). The asymmetry in the coupling between the electrode and the carbon atom in the carbon chain becomes the reason for a variation in the transmission channel within the bias window and that gives rise to NDR for the device structure (Khoo et al., 2008). It is also observed by researchers that a bias dependent frontier orbital rearrangement causes NDR in the device (Zhou et al., 2008). A change in phase of the broken symmetry wave function also believed to lead to nonlinearity in the I-V characteristic and eventually to the NDR behavior (Pati et al., 2008). It has been shown that in a squashed C<sub>60</sub> molecule the frontier orbitals would have made less contact with the electrodes, which translates as weak coupling with the contacts and becomes the reason for NDR in the device (Fan et al., 2008). The charge redistribution in the molecule in the forward and reverse voltage bias is believed to be the reason for NDR in some of the single molecule devices (Min et al., 2010). In a carbon-based molecular device, it is shown that the NDR is due to the suppression of conduction orbitals (Wan et al., 2012), and a similar kind of response is observed from a molecule which is dependent on the number (odd/even) of carbon atoms in the spacer chains (Mahmoud and Lugli, 2013; Zhang et al., 2013).

Even after such rich theoretical understanding of the principle of NDR, there still exists a vacuum when we try to correlate the experimental observations from similar kind of experimental setup and hence the universal explanation of NDR for any device is still illusive and the pursuit of understanding the principle of NDR is still on. In this work for the first time we have tried to explain a multi NDR feature on both the voltage bias directions from a device consisting of a redox molecule by using first principle calculation using density functional theory (DFT) combined with non-equilibrium Green's function (NEGF). The molecule chosen for this purpose is DDQ which shows redox behavior (Bandyopadhyay and Pal, 2003a) and also possess the property of charge transfer complex formation (Rath et al., 2008), because of these behaviors this molecule has been used in many studies related to memory device application (Bandhopadhyay and Pal, 2003; Mukherjee and Pal, 2004; Vyas et al., 2018). Hence, we have tried to utilize these properties of the molecule in our study as well. We have shown that the NDR feature is observed on both positive and negative voltage bias and we explained the phenomenon on the basis of a competing act of double reduction of the molecule and the interface resistance between the molecule and the electrodes.

## 4.2 Experimental

### 4.2.1 Computational methodology

For studying the frontier orbitals of the neutral, singly reduced, and doubly reduced molecule we used Gaussian 09W. The device structure used for the simulation is the following: a 2,3-Dichloro-5,6-dicyano-1,4-benzoquinone (DDQ) molecule is connected between two similar gold (Au) 111 electrode, where the oxygen atoms in 1 and 4 positions of the benzene ring are connected directly to the gold atom of the electrodes. The schematic of the device is shown in Fig. 4.1(a). In this device the central scattering region is spread between first 3 layers of Au atoms from the left electrode, the molecule under test and the first 3 layers of Au atoms in the right electrode. The first principle self-consistent calculation on the device is performed by considering

the above device architecture. DDQ molecule was optimized by using DFT before it is connected to the left and right electrodes. The device is then energy relaxed with the help of Quasi Newton Method till the maximum force between all atoms in the molecule is reduced to 0.005 eV/Å and maximum stress between atoms are also reduced to 0.005eV/ Å<sup>3</sup>. The most inter atomic force relaxed device structure was obtained at gold-oxygen bond-length of 2.266 Å on left junction and 2.268 Å on right junction with 132.804° between gold-oxygen-carbon on left and 132.144° between gold-oxygen-carbon atom on right junction. After geometry relaxation DDQ molecule loses very little planarity. The vector projection of DDQ molecule on Au <111> plane is nearly perpendicular. So, the charge transport in the device was studied by using a combination of density functional theory (DFT) and non-equilibrium Green's function (NEGF). This was carried out by using Atomistic Tool Kit (VNL ATK 2014.3) (Brandbyge et al., 2002; Taylor et al., 2001). Here the charge transport in the device is along the z-direction, hence the k-point sampling is chosen accordingly. The Poisson equation is solved by keeping a density mesh cut-off energy of 75 Hartree. The basis set used are double zeta polarized for molecule atoms and single zeta polarized for gold electrodes atoms. Local Density Functional (LDA) is used in the formulation of Perdew Zunger (PZ) (Perdew and Zunger, 1981) exchange correlation functional where Dirac Bloch being the exchange functional and Perdew Zunger being the correlation functional. The electron temperature is kept at 300 K. The I-V characteristic and the transmission spectrum for the device is calculated by using Landauer equation (Büttiker et al., 1985):

$$I(V) = \frac{2e}{h} \int_{\mu_R}^{\mu_L} dE T(E, V) [f_L(E) - f_R(E)] \quad (4.1)$$

In the above equation, e and h are electronic charge and plank's constant, V is applied bias which is equal to  $\frac{\mu_L - \mu_R}{e}$ .  $\mu_L = E_f + \frac{eV}{2}$  and  $\mu_R = E_f - \frac{eV}{2}$  are chemical potentials at left and right contacts respectively,  $E_f$  is the energy of the fermi level.  $f_L$  and  $f_R$  are Fermi functions described as:  $f = \frac{1}{(1 + e^{(E - \mu)/kT})}$ . The transmission coefficient which is a function of energy (E) and applied bias (V) can be calculated from the following equation:

$$T(E, V) = Tr[\Gamma_L G \Gamma_R G^\dagger] \quad (4.2)$$

Where G and G<sup>†</sup> are the retarded and advanced Green's functions respectively from the scattering region.  $\Gamma_{L(R)} = i(\Sigma_{L(R)} - \Sigma_{L(R)}^\dagger)$  is the coupling function for the end of scattering region with the left and right electrodes,  $\Sigma_{L(R)}$  and  $\Sigma_{L(R)}^\dagger$  are the self-energies given as  $\Sigma_{L(R)} = \tau_{L(R)}^\dagger g_{L(R)} \tau_{L(R)}$  and  $\Sigma_{L(R)}^\dagger = \tau_{L(R)}^\dagger g_{L(R)}^\dagger \tau_{L(R)}$ . Here  $g_{L(R)}$  is the Green's function for normal contact and is calculated using the periodicity of the contact,  $\tau_{L(R)}$  describes the interaction between the molecule and the left (right) electrode. So, the contacts add self-energies to the device Hamiltonian and the total Hamiltonian becomes  $H = H_d + \Sigma_L + \Sigma_R$ , where  $H_d$  is the device Hamiltonian without contact and is explicitly included in the Kohn-Sham calculation for the total system.

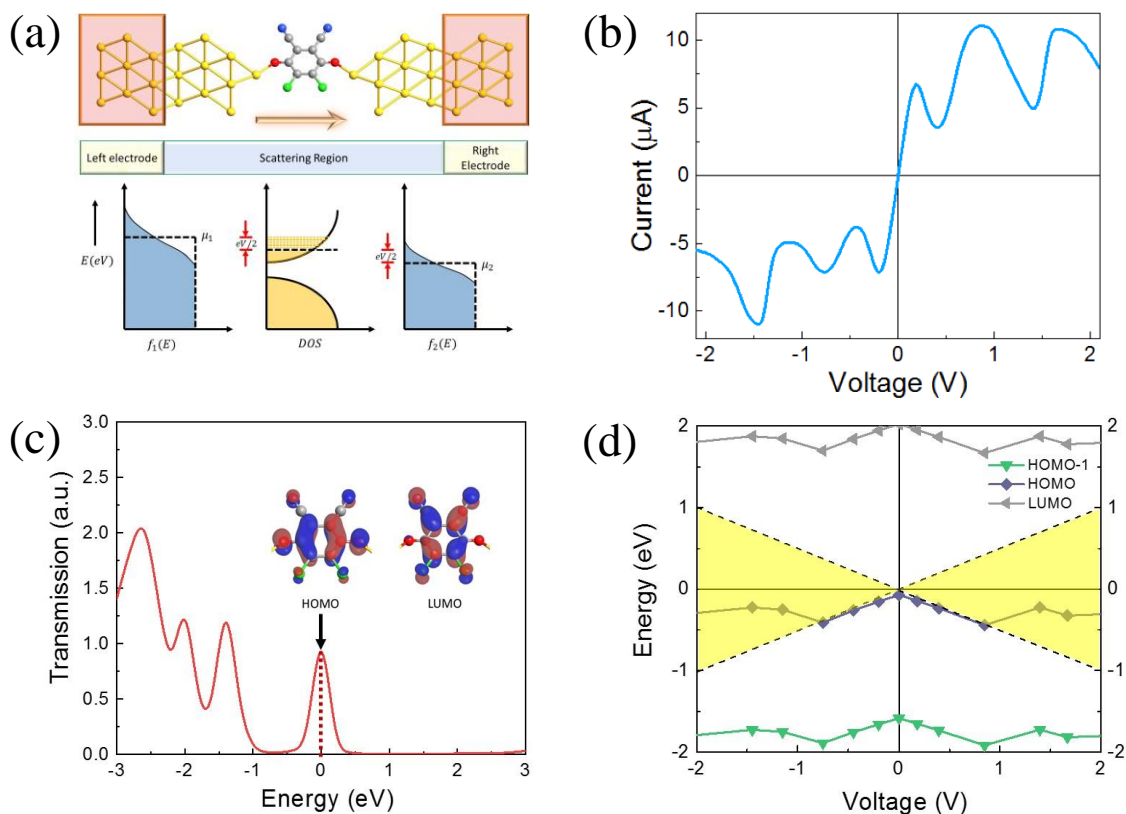


Fig. 4.1. (a) The schematic diagram of gold-DDQ-gold device. A schematic representation of the energy level distribution in the electrodes and the molecule is also shown below it. (b) The I-V characteristic curve for the device. (c) Transmission spectrum at zero bias from the device. (d) The HOMO, LUMO, and HOMO-1 levels with the change in voltage. The shaded region within the dotted line represents the energy window corresponding to the voltage bias of interest (-2 to 2 V).

#### 4.2.2 STM Study

To study the devices experimentally we characterized the devices using an ultra-high vacuum scanning tunneling microscope (UHV-STM) from Omicron. The devices were prepared by in situ e-beam deposition of DDQ molecules on gold (Au) 111 substrate. The Au 111 substrate was procured from SPI supplies and was annealed at 300 °C for 30 mins before deposition of the molecule. The deposition rate was controlled in a way that only a monolayer of material deposited on the substrate. After the deposition the device was characterized at room temperature and  $10^{-10}$  mbar pressure using an electrochemically etched platinum-iridium (Pt-Ir) tip.

### 4.3 Results and Discussions

#### 4.3.1 Theoretical I-V study and zero bias transmission

The I-V characteristic curve from the device was obtained in a voltage window of -2.5 to 2.5 V by using a self-consistent calculation but we are focusing only on the range between -2 to 2 V and is shown in Fig. 4.1(b). In I-V analysis, a  $10 \times 10$  grid of k-points is used to sample the Brillouin zone as Monkhorst-Pack grid (Monkhorst and Pack, 1976) from energy range of -10 eV to 10 eV. The I-V characteristic curve is nonlinear on both the sides and having multiple negative differential resistance (NDR) peaks. The corresponding voltages for peaks and valleys are mentioned in table-4.1 along with the peak to valley ratios.

Table 4.1. The peak and valley voltages, currents along with the peak to valley current ratio (PVR) in both positive and negative side.

$V_{peak}$ (V)		$V_{valley}$ (V)		$I_{peak}$ ( $\mu$ A)		$I_{valley}$ ( $\mu$ A)		$I_{peak}/I_{valley}$	
+ve	-ve	+ve	-ve	+ve	-ve	+ve	-ve	+ve	-ve
0.186	-0.20	0.40	-0.45	6.72	-7.14	3.55	-3.8	1.91	1.88
0.87	-0.75	1.41	-1.15	11.06	-7.11	4.98	-4.92	2.24	1.44
1.65	-1.45	2.16	-2.10	10.79	-10.95	7.77	-5.51	1.39	1.99

It can be seen from the I-V curve that the current increases linearly and rapidly from 0 to the order of  $10^{-6}$  A on both positive and negative directions within 0.2 V and this can be ascribed to the resonant tunneling at low voltage bias (Nitzan, 2001; Zheng et al., 2010). In the positive direction the peak current increases till the second NDR peak but for the third peak the magnitude of current decreased. The trend was maintained for the peak to valley current ratio ( $I_{P/V}$ ) as well where it increased from first to second NDR peak but for the third one the current came down. While in the negative direction the peak current first decreases and then increases from first to third peak. The trend is followed in  $I_{P/V}$  as well. The maximum  $I_{P/V}$  obtained from the curve is 2.2. To understand the electronic transport in the system it is important to look at the spatial distribution of the molecular orbitals at zero bias, so in Fig. 4.1(c) we have shown the eigen states corresponding to the Highest Occupied Molecular Orbital (HOMO) and the Lowest Unoccupied Molecular Orbital (LUMO), which were calculated by using a self-consistent method involving both the molecule and the electrodes such that the interaction between the two of them was included in the Hamiltonian. The frontier orbitals show contrasting distribution of orbital over various atoms. At zero bias the orbitals are not localized over the oxygen atoms for the LUMO level but are localized for the HOMO level. The localization over other functional groups in the molecule is mostly restricted to the LUMO. The zero-bias transmission from the device suggests that the transport and tunneling in the device is mainly through the HOMO of the molecule. Due to the difference in the electronegativity of the oxygen atom at the end of the molecule and the gold atom of the electrode the charge density will be more localized towards the oxygen atom which is evident from the HOMO of the molecule, and because of this the HOMO is aligned with the fermi level.

We expect the molecular orbitals to evolve with applied bias and which indeed is happening and can be seen in Fig. 4.1(d). The bias window corresponding to the energy is shown by the shaded area within the dotted line. Here we have plotted the energy corresponding to the LUMO, HOMO, and HOMO-1 orbitals at different biases. As seen from the figure only the HOMO of the molecule falls within the energy window and that explains why HOMO is responsible for the transport of electrons. The other two orbitals are shown for reference purpose. Each data point in the figure is corresponding to either peak or valley voltage obtained from the I-V characteristic curve. The HOMO level on both positive and negative voltage biases go parallel to the dotted line till 0.39 V on the positive side and -0.44 V on the negative side. At 0.84 V on the positive side and -0.77 V on the negative side the HOMO level partially entered into the bias window and at this point the HOMO and LUMO gap (HLG) is the minimum. Till this point the HOMO level moves away from the Fermi level but at 1.42 V and -1.13 V the HOMO level has completely entered into the energy window and moved towards the Fermi level. As it enters into the energy window the current decreases at 1.42 V and -1.13 V. These features are observed because as the device is scanned at different applied bias the system will no longer be in equilibrium and the molecular energy levels will shift. The reasons for this could be the continuous change in electron density of the molecule or change in the coupling strength between the electrodes and molecule (Zhang et al., 2013).

### 4.3.2 Experimental I-V characterization

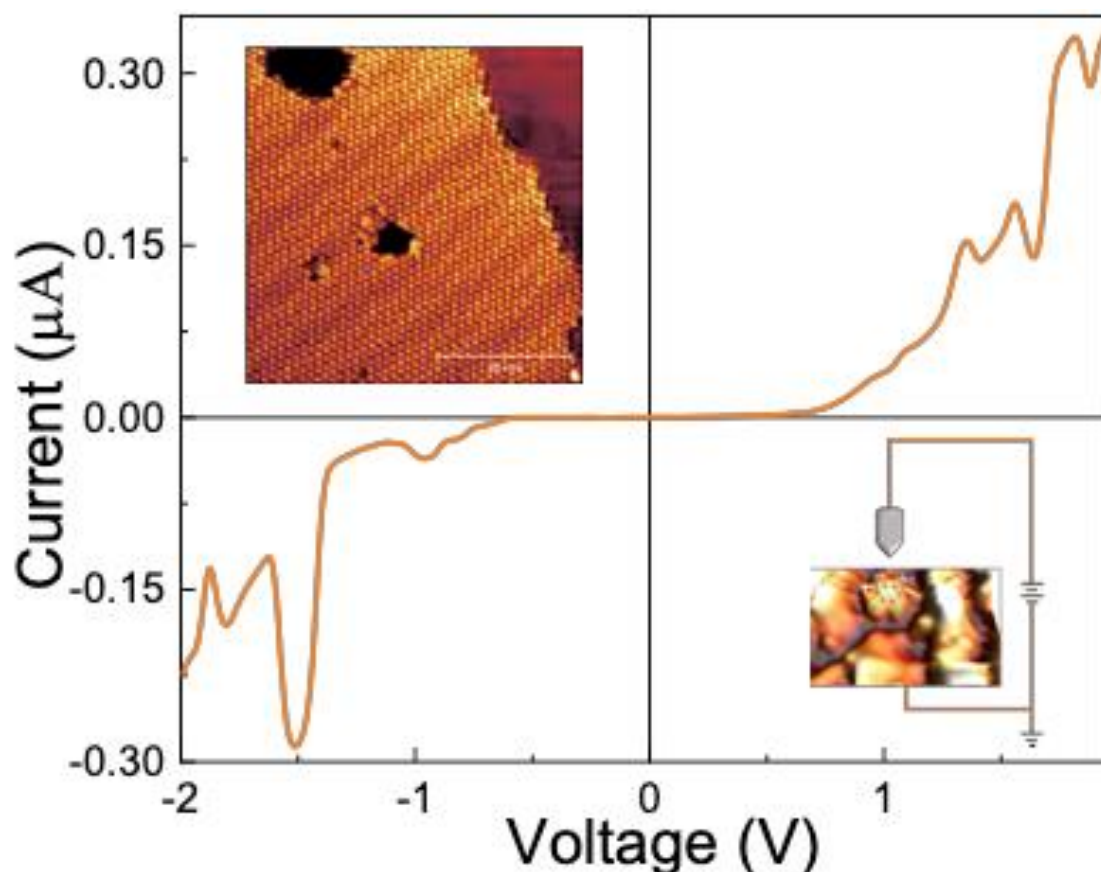


Fig. 4.2. The experimental I-V curve from an Au/DDQ/Pt-Ir device configuration studied. The upper inset shows an STM image of a 50 x 50 nm<sup>2</sup> area scan of the DDQ molecule deposited gold <111> surface. The lower inset shows the schematic of the study of a single DDQ molecule under the STM tip.

To study the experimental I-V curve we observed the DDQ deposited Au substrate. The surface is covered with a uniformly arranged layer of DDQ molecule as shown in the upper inset of Fig.4.2. The schematic of studying the single DDQ molecule is shown in the lower inset of the same figure. As can be seen from the figure there exists a single DDQ molecule under the sharp tip. The ball and stick model of the molecule is overlapped over the DDQ molecule to understand the orientation of the molecule present on the surface. The surface was scanned at a gap voltage of -1 V and a set point current of 500 pA. To study the I-V characteristic of the single molecule in  $\pm 2$  V range we probed every part of the molecule and recorded thousands of I-V curves. Statistically the majority of the I-V curves looked like the one showed in Fig. 4.2. There exist multiple NDR peaks on both the sides of I-V curve. Since we are probing the molecule using a tunneling mechanism the NDR peaks are observed at different locations (1.37 V, 1.58 V, 1.84 V, and -0.97 V, -1.53 V, -1.83 V) along the voltage axis in comparison to the theoretically calculated I-V curves. Within  $\pm 1$  V range there is hardly any current and this is because for the current to flow a threshold energy is needed for the electron to tunnel through the vacuum barrier and perhaps that is happening only after this voltage range. Moreover, the work function of the two metal electrodes is different because of the difference in the used electrode materials as opposed to the electrodes used for theoretical calculations.

### 4.3.3 Transmission spectra and LDDOS

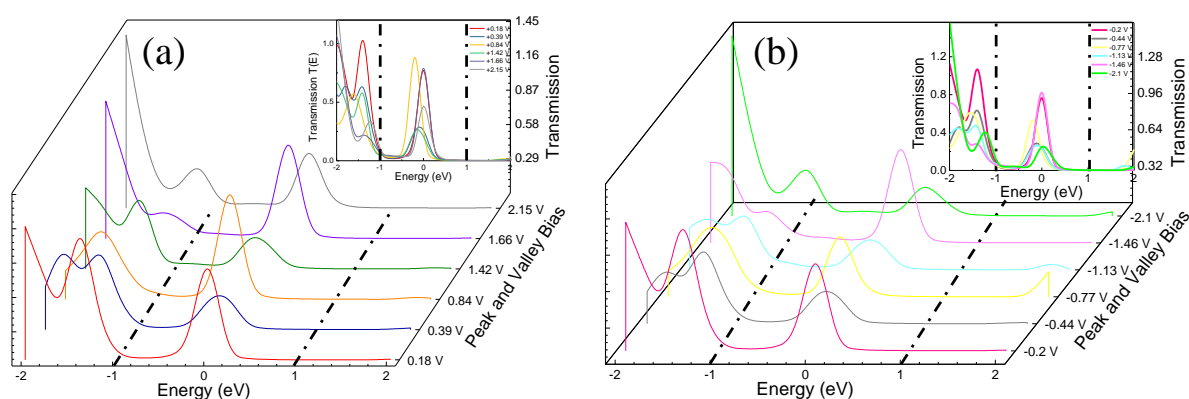


Fig. 4.3. (a) The transmission spectra from the device at positive peak and valley voltages. The peak voltages are 0.18 V, 0.84 V, and 1.66 V whereas the valley voltages are 0.39 V, 1.42 V, and 2.15 V respectively. The inset shows the normalized spectra for positive peak and valley voltages. (b) the transmission spectra from the device at negative peak and valley voltages. The peak voltages are -0.2 V, -0.77 V, and -1.46 V whereas the valley voltages are -0.44 V, -1.13 V, and -2.1 V respectively. The inset shows the normalized spectra for negative peak and valley voltages. The dot-dashed lines in all the figures encompass the energy window. The inset images are further explained in Appendix B1.

To understand the simulated I-V curve better, the transmission spectra of the molecule was studied at different applied bias corresponding to the peaks and valleys in the I-V curve, and the area under the transmission curve within the energy window gives the information about the total current through the device. The transmission peaks in the positive bias in Fig. 4.3(a) corresponding to the peak voltages coincide with the HOMO energy level except for +0.84 V, which is shifted a little bit to the left of the fermi level. For valleys, the peak for 2.15 V is at the fermi level but for 0.39 and 1.42 V they are away to the left of the fermi level. This resonant shift of the transmission peak is may be due to the change in electronic structure leading to selectivity of transmission channels at a particular bias (Li and Kosov, 2006). The change in the transmission spectra is due to the change in polarization of the molecule with applied bias and the position of the transmission peak is related to the energy of the associated molecular orbital (Kaasbjerg and Flensberg, 2008; Zhang et al., 2013). In Fig. 4.3(a) it is clear that the area under the curves corresponding to the peak voltages is much higher than the area under the curves corresponding to the valley voltages within the energy range (dash dotted line). The way I-V curve is symmetrical in both forward and reverse bias except having different peak and valley positions on both the sides, the nature of the transmission curves for both positive and negative sides is also similar and can be seen in Fig. 4.3(b), meaning the area under the transmission spectra within the energy window is more for the peaks than the valleys. This is because the strength of the transmission peak is associated with the extent of delocalization of the orbitals. The normalized transmission spectra for both the positive and negative NDR peak and valley voltages are shown in the inset of both Fig. 4.3(a) and (b).

The Local Device Density of States (LDDOS) is the projection of the device density of states at the fermi level (Li et al., 2018) and for the device it explains the extent of overlapping between the states contributing towards the integral current across the device. In our device it is spread only in a small region around the fermi level which is corresponding to the HOMO of the molecule. As can be seen in Fig. 4.4 for both positive and negative bias the LDDOS within the energy window is more for the peak than the valley voltages. With increase in bias the DOS for the molecule concentrated at the bottom of right-hand electrode for positive bias and on the bottom of left-hand electrode for negative bias. This means even the states below HOMO are participating in the transmission.

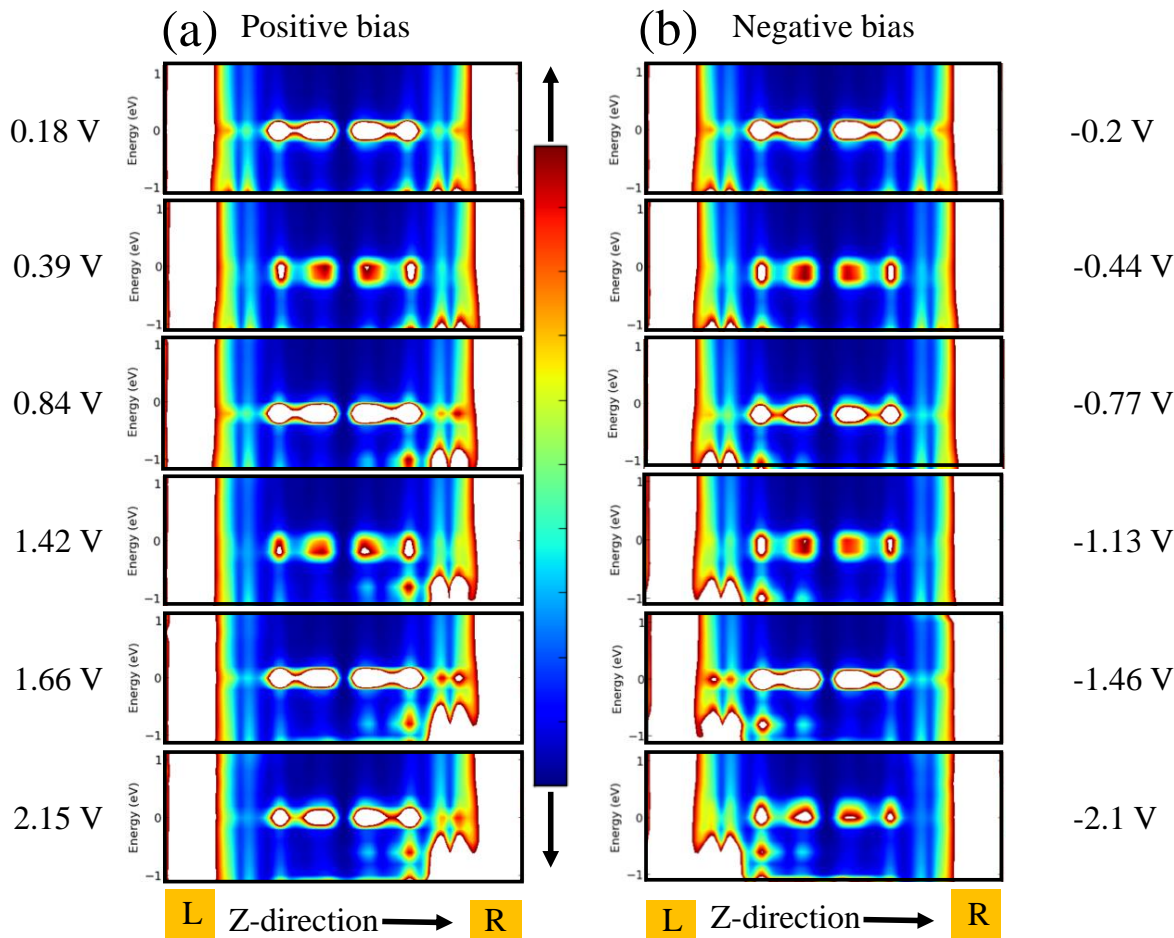


Fig. 4.4. (a) and (b) represent the local device density of states (LDDOS) for positive and negative peak and valley voltages. The electrodes are represented by the yellow blocks at the bottom with L and R written on them, representing the left and right electrodes respectively.

#### 4.3.4 Molecular Projected Self Consistent Hamiltonian (MPSH) orbitals study

The eigen states corresponding to the peaks and valleys in both positive and negative sides of the I-V curve are shown in Fig. 4.5(a) and (b). The eigen states in the positive side for first peak and valley at 0.18 V and 0.39 V in Fig. 4.5(a) have shown almost the similar type of spatial orbital overlapping, but a close comparison of the two tells that there is a difference in phase in their orientation. For both the peak and valley the overlapping of orbitals is extent from one end to the other end of the scattering region. For the next peak voltage (0.84 V), the current is high through a completely different spatial orbital overlapping, and this time the overlapping was restricted to the left electrode only. For the ensuing valley as we can see though the overlapping is same but there is a difference in the phase of orientation. Again, the third peak (1.66 V) has a different type of orbital overlapping which might have led to a higher current flow through the device. In this case the overlapping is end to end in the scattering region. The valley at 2.15 V has a different type of orbital overlapping which is restricted to the left electrode only.

For the negative direction we can analyze the peaks and valleys by using similar type of analogy. The peak at -0.2 V and valley at -0.44 V are result of difference in phase of orientation of the overlapped orbitals. For the next pair of peak (-0.77) and valley (-1.13) the orbitals are overlapped in the similar way as in the previous case but clearly the difference in the phase of orientation is what causes the high and low current values. For the last pair of peak (-1.46) and valley (-2.1) the overlapping is completely different than the previous two cases, but amongst themselves there is a clear difference in phase of orientation.



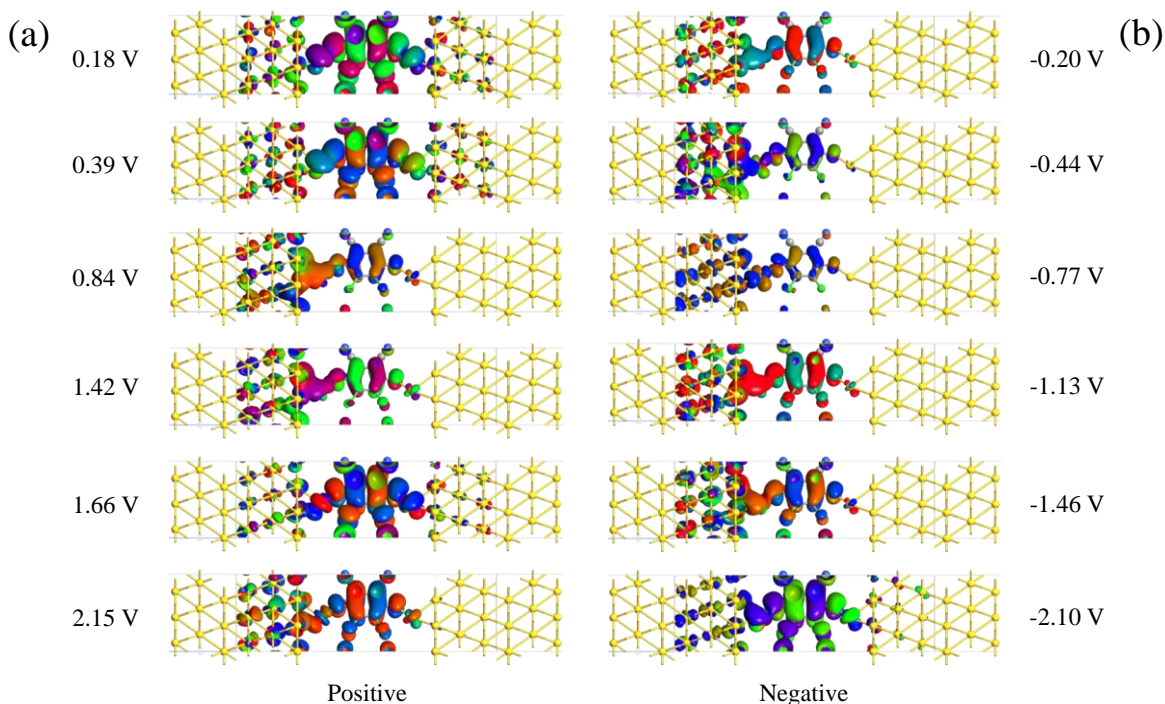


Fig. 4.5. (a) and (b) represent the eigen states of MPSH for the positive and the negative peak and valley voltages. The peak and valley voltages in the positive side are 0.18 V, 0.84 V, 1.66 V and 0.39 V, 1.42 V, 2.15 V respectively. Similarly, for the negative side the peak and valley voltages are -0.2 V, -0.77 V, -1.46 V and -0.44 V, -1.13 V, -2.1 V respectively.

In the negative direction for most of the bias voltages the overlapping was mostly restricted to the left electrode. So, the difference in LDDOS and MPSH is that LDDOS focuses mainly on the contributing states but does not show the microscopic picture but MPSH shows the picture in microscopic scale as it shows the projection of the orbitals corresponding to the eigen state. To check whether the presence of the electronegative functional group (oxygen) leads to the appearance of NDR peaks, we performed simulation on devices consisting of a singly or a doubly reduced molecule.

#### 4.3.5 Characteristics of singly and doubly reduced DDQ molecule

Before making the connection with the electrodes the molecule was first singly reduced by donating one electron to the neutral molecule such that the number of charges in the molecule has now becomes 113 in comparison to 112 in neutral DDQ structure and then optimized. The electron was localized mostly over the oxygen atoms which can be seen from the charge density plot in the right-hand side bottom inset of Fig. 4.6(a). The device made from this molecular structure with two gold electrodes was studied under the same conditions as the neutral molecule and the bond-length between gold and oxygen at left electrode-molecule junction is 2.20948 Å while at right end it is 2.20945 Å but bond-angle between gold-oxygen-carbon raised to 142.179° at left junction while 142.183° at right end. The I-V characteristic curve is symmetric and shows an NDR peak and valley at 1 V and 1.5 V in the positive side and at -1 V and -1.5 V in the negative side. In addition to that there also exists a small hump, which is clearly visible in the differential conductance plot (green arrows) shown in the top left inset of Fig. 4.6(a). The differential conductance plot shows the maximum at 0 V, this is because of the steep increase in the current at low bias (Li and Kosov, 2006). The green arrows in the conductance plot show the dip due to the hump in the I-V curve at  $\pm 0.47$  V and the yellow arrows are representing the dips due to NDR peaks on both the sides.

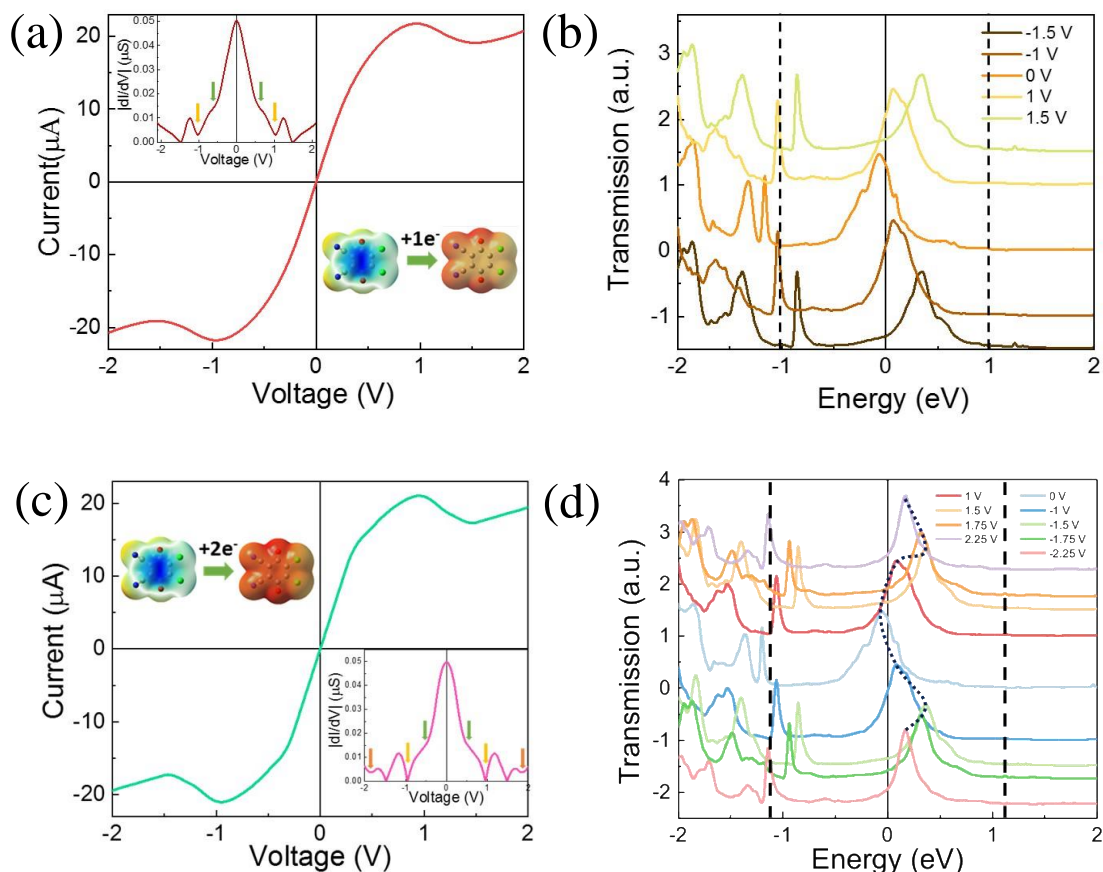


Fig. 4.6. (a) I-V characteristic curve of a device having singly reduced DDQ molecule. The top inset shows the plot for conductance variation with respect to the voltage. The bottom inset shows the charge density of the neutral and singly reduced molecules. (b) the transmission spectrum from the device consisting of singly reduced molecule (c) I-V characteristic curve of a device having doubly reduced DDQ molecule. The top inset shows the charge density of the neutral and doubly reduced molecules. The bottom inset shows the plot for conductance variation with respect to the voltage. (d) the transmission spectrum from the device consisting of doubly reduced molecule.

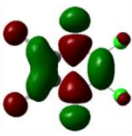
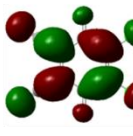
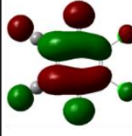
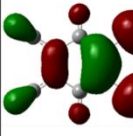
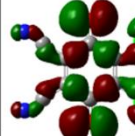
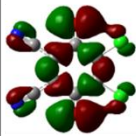
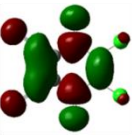
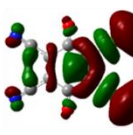
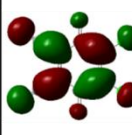
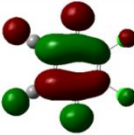
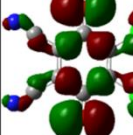
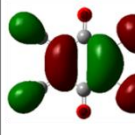
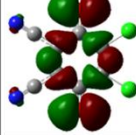
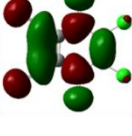
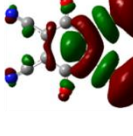
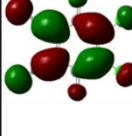
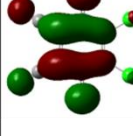
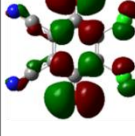
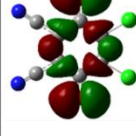
The transmission spectrum from this device is shown in Fig. 4.6(b). The spectrum is obtained at the peak and valley voltages. At zero bias the peak corresponding to the HOMO is just left to the fermi level because the molecule is already polarized by reduction (Kaasbjerg and Flensberg, 2008), but when the voltage increases in the positive side the peak shifts to the high energy region and for 1.5 V a new peak showed up on the left-hand side within the energy window (dotted lines). The transmission spectra for the negative bias also follow the same trend with a new transmission peak showing up for -1.5 V in the energy window. The behavior of the transmission spectra for the positive and negative bias direction is identical. The magnitude of transmission is more at the NDR peak voltages than the valley voltages. This also tells us that though two channels are available for transmission in high voltages it is the area under the curves for the peak voltages which is more than the valley voltages and hence more current flows at the peak than at the valley voltages. The extra transmission peak for  $\pm 1.5$  V within the bias window leads to relatively larger current than the neutral molecule and hence smaller peak to valley ratio. This also validates the observation from LDDOS, where at higher voltages the energy levels below HOMO were also participating in transport.

Now the doubly reduced molecule was prepared by donating two electrons to the neutral molecule such that the number of electrons has increased from 112 to 114 and then energy optimized before making the connection with the two gold electrodes. As can be seen in the upper left-hand side inset of Fig. 4.6(c), the electrons are mostly localized over the two oxygen atoms. Similar to singly reduced DDQ molecule, bond-length between gold and oxygen reduced to

2.21524 Å on left junction and 2.21503 Å on right junction for the doubly reduced DDQ. For this structure the bond-angle between gold-oxygen-carbon is 141.715° at left interface and 141.697° at right interface. The corresponding I-V curve is shown in Fig. 4.6(c). The nature of the I-V curve is very similar to the singly reduced molecule based device with a small difference i.e. there are two NDR peaks, one is prominent in the I-V curve but the other one is distinctly seen in the differential conductance plot which is shown in the lower inset of Fig. 4.6(c). In the conductance plot there are two dips on both the sides of origin shown by yellow and orange arrows at both positive and negative values of 1 V and 1.75 V. A shoulder in the I-V curve at 0.47 V gives rise to a small dip shown by the green arrows in the conductance plot.

The transmission spectra for the device is shown in Fig. 4.6(d). The zero bias spectrum along with the spectra at  $\pm 1$  V and  $\pm 1.5$  V have not changed at all in comparison with the singly reduced structure. For the next peak and valley voltages the peak position has shifted to the left towards the zero bias peak position. It is observed that the area under the transmission curve is more for the peak voltages than the valley voltages. These features are identical in the negative side as well and the peak shifting from the negative to the positive voltage bias follows a wave like selectivity of transmission channel shown by the dotted line. The coupling strength of the molecule varies with the increase in voltage in positive and negative sides.

Table 4.2. The frontier orbitals along with the higher (LUMO+1, and LUMO+2) and lower (HOMO-1, and HOMO-2) orbitals of neutral, singly, and doubly reduced molecules of DDQ and a SOMO for the singly reduced DDQ.

Type of Orbital	LUMO+2	LUMO+1	LUMO	SOMO	HOMO	HOMO-1	HOMO-2
Type of molecule							
Neutral							
Singly reduced							
Doubly reduced							

To correlate the transmission spectra with the orbital orientation of the molecule, we studied different orbitals including the frontier orbitals of the neutral, singly, and doubly reduced molecule without the contacts, and is shown in table 4.2. The orbitals are differently oriented for the HOMO and LUMO of the molecule in all the three cases. The HOMO-1 and HOMO-2 for the neutral molecule are different and diffused than the HOMO. Similarly, the LUMO+1 and LUMO+2 are also different than the LUMO. For the singly reduced molecule the LUMO is completely different from the LUMO of neutral molecule. The HOMO-2 and the LUMO+1 are completely different from the corresponding levels for neutral molecule. For the doubly reduced molecule LUMO is same as the corresponding singly reduced molecule but it is different from the LUMO of neutral molecule. The HOMO and HOMO-1 of the doubly reduced molecule are different from that of the singly reduced molecule. But in comparison with neutral molecule the

HOMO-2 is slightly different but the LUMO+1 is completely different. As it was observed from the transmission spectra for singly and doubly reduced molecules that the peaks within the bias window are shifting toward the positive energy region at higher bias, so we can say that the transport through these molecules is predominantly through the LUMO and higher levels. It can be seen from table 4.2, indeed the LUMO and LUMO+1 energy levels are different for the reduced structures in comparison to the neutral structure. We also saw that at some higher biases ( $\pm 1.5$  V for singly reduced molecule and  $\pm 1.5$  V and  $\pm 1.75$  V for doubly reduced molecule) few more sharp transmissions peaks showed up in the energy window. We can associate these peaks to the HOMO-2 orbitals.

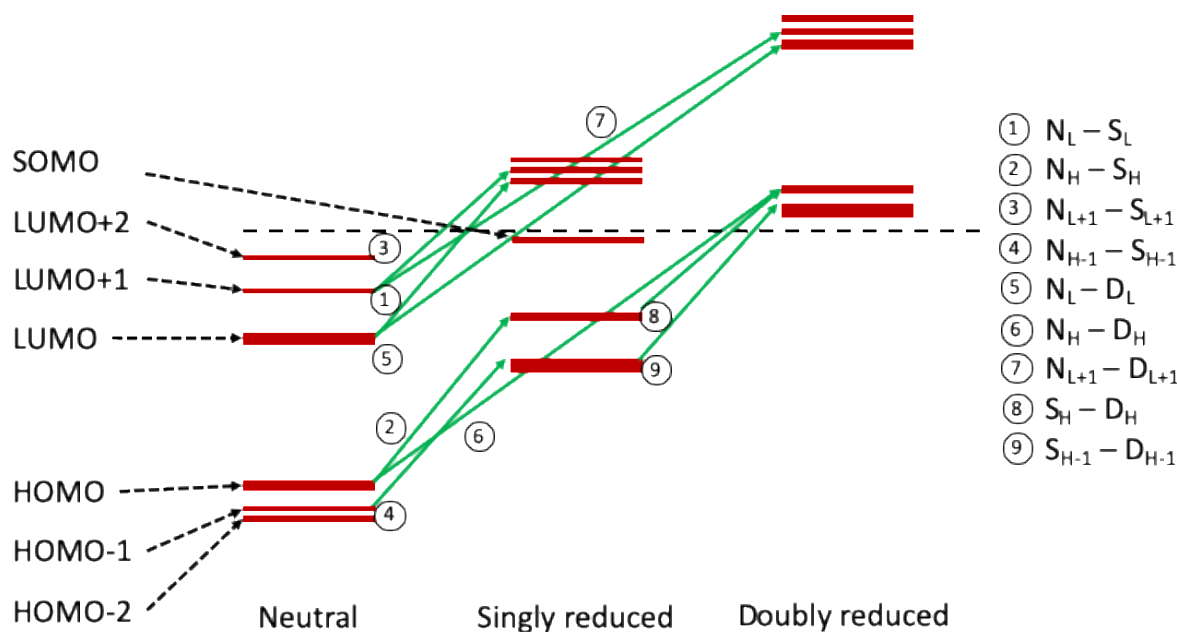


Fig. 4.7. The various possible molecular transitions between the neutral, singly, and doubly reduced DDQ molecules orbitals are shown by the numbers from 1 to 9 and represented by the green arrows. Here the abbreviation used for neutral, singly reduced, and doubly reduced molecules are N, S, and D respectively.

So, the allowed change in orbital orientation with the reduction of the molecule is shown in Fig. 4.7. As can be seen, energetically the molecule prefers to be in neutral state than the singly or doubly reduced molecular structure, but the HOMO-LUMO gap first increases in the singly reduced molecular structure and then decreases for the doubly reduced structure, which is the reason for variation in transport through the molecule (Seminario et al., 2000). The transitions observed in various orbital orientation are shown by green arrows. The numbers 1 to 9 represent the paths where the orientation of the orbitals change, which may contribute to the change in the resistance of the device.

#### 4.4 Analysis

In our devices the NDR phenomenon with multiple NDR peaks in both positive and negative voltage bias is an interesting observation. Here the NDR is a voltage controlled multiple N type effect. We attribute the NDR effect of the device to two competing factors, i.e. the interface between the molecule and the electrode, and the reduction of the molecule. These two things are clear from the MPSH eigen states corresponding to the peak and valley voltages shown in Fig. 4.5. Since from the MPSH orbitals we can perceive that at 0.18V the orbitals are spread to both the electrodes in the scattering region, hence there is no role played by the interface and we can represent the NDR peak at 0.18 V to the reduction of one of the oxygen atoms by gaining an electron. Once the electron is trapped by the oxygen atom, the energy levels for this electron will be quantized and the electron will remain in the quantum state till it gets a resonant energy, which

happens at 0.39 V and hence the current started increasing as observed in the I-V curve. The reduction of the molecule at around 0.18 V can be verified by the cyclic voltammetry data (Hamid et al., 2009). For the singly reduced molecule we saw that the peak due to reduction is not present and the small dip in the differential conductance can correspond to the onset of current after the valley. The peak is absent because the molecule was already reduced prior to the connection with the two electrodes. Once the current starts increasing it reaches a maximum at 0.84 V and afterwards it starts decreasing and is apparent from the eigen states figure, which shows that at this voltage the molecular orbitals are concentrated only on the left electrode and there is hardly anything on the right electrode. This suggests that the contact resistance between the molecule and the right electrode is more which results in the decrease in current in the device even at 1.42 V (Fan and Chen, 2010; Shi et al., 2005). For the singly and doubly reduced molecules, the NDR peak was obtained at 1 V and from there on the current decreases till 1.5 V. There is a small difference in the peak and valley positions for the singly and doubly reduced molecule-based devices in comparison to the neutral molecule-based device, and this could be due to the difference in contact resistance of these molecules with the electrodes.

After 1.4 V the current started increasing till 1.66 V and from Fig. 4.5 it is clear that the orbitals are spread more or less equally on both the electrodes at this voltage, which means the resultant peak is not an effect of contact resistance but something else. Incidentally the molecule possesses another oxygen atom which can also be a site for the localization of electron. So, the molecule can be reduced by a second electron which leads to the appearance of quantized energy levels for the second electron and unless it received a resonant energy, it will not be free for transport. Therefore, the second reduction of the molecule occurs at 1.66 V and stays in the low conducting state even beyond 2 V. Here we have shown that even at 2.25 V the current stays low. In the device consisting of the doubly reduced molecule no NDR peak was observed in the I-V curve due to reduction as the molecule was already reduced twice. The dip at 1.75 V is due to the onset of the current after the valley due to reduction, which was not visible. In the negative direction of voltage scan also we observed NDR peaks and valleys and from Fig. 4.5 we can say that they are not only due to the oxidation of the molecule but all of them are due to the interplay of oxidation and contact resistance between the molecule and the electrodes.

## 4.5 Conclusion

Multiple NDR peaks in the I-V curve on both positive and negative sides of a single DDQ molecule-based device was observed. The NDR phenomenon was attributed to two competing factors, one; due to the double reduction of the molecule which leads to change in the conformation of the molecule, and second; the contact resistance between the molecule and the electrodes at certain bias voltages. The increase and decrease in the current at the peak and valley voltages were explained by using the transmission spectra corresponding to the HOMO of the molecule. This explanation of NDR effect was also validated by considering the singly and doubly reduced molecule. The multiple bidirectional NDR effect from the device was also verified by studying single molecule in scanning tunneling microscope and indeed at room temperature the device showed multiple NDR peaks on both the sides of the I-V characteristic curve.

